Mammalian Genome 9, 20–25 (1998).

Mammalian Genome
Incorporating Mouse Genome
© Springer-Verlag New York Inc. 1998

A new mutation *Rim3* resembling Re^{den} is mapped close to retinoic acid receptor alpha (*Rara*) gene on mouse Chromosome 11

Hajime Sato,[1,2] Tsuyoshi Koide,[2] Hiroshi Masuya,[2] Shigeharu Wakana,[3] Tomoko Sagai,[2] Akihiro Umezawa,[4] Sei-ichi Ishiguro,[1] Makoto Tama,[1] Toshihiko Shiroishi[2]

[1]Department of Ophthalmology, Tohoku University School of Medicine, Seiryo-Machi 1-1, Sendai, Miyagi-ken 980, Japan
[2]Mammalian Genetics Laboratory, National Institute of Genetics, Yata 1111, Mishima, Shizuoka-ken 411, Japan
[3]Central Institute for Experimental Animals, Miyamae-ku, Kawasaki 216, Japan
[4]Department of Pathology, Keio University School of Medicine, Shinanomachi 35, Shinjuku-ku, Tokyo 160, Japan

Received: 3 July 1997 / Accepted: 26 August 1997

Abstract. A new mouse mutation, recombination-induced mutation 3 (*Rim3*), arose spontaneously in our mouse facility. This mutation exhibits corneal opacity as well as abnormal skin and hair development resembling rex denuded (Re^{den}) and bareskin (*Bsk*). Large-scale linkage analysis with two kinds of intersubspecific backcrosses revealed that *Rim3* is mapped to the distal portion of Chromosome (Chr) 11, in which Re^{den} and *Bsk* have been located, and is very close to the retinoic acid receptor, alpha (*Rara*). The genes, keratin gene complex-1, acidic, gene 10, 12 (*Krt1-10, 12*), granulin (*Grn*), junctional plakoglobin (*Jup*) and *Rara*, all of which regulate growth and differentiation of epithelial cells, are genetically excluded as candidate genes for *Rim3*, but are clustered in the short segment on mouse Chr 11.

Introduction

Early reports described linkages between keratin genes and mouse mutants with abnormal skin and hair development. Keratin gene complex-1, acidic (*Krt1*) is located on the distal portion of Chr 11, where the mutations rex (*Re*), *Bsk*, and Re^{den} are co-localized, while keratin gene complex-2, basic (*Krt2*) is located on the distal portion of Chr 15, where the mutations caracul (*Ca*), shaven (*Sha*), velvet coat (*Ve*), and naked (*N*) are clustered (Green 1989). These tight linkages suggested that keratin genes are plausible candidates for the mutations. Among these mutations, Re^{den} and *Bsk* exhibit corneal opacity as well as abnormal skin and hair development. *Re* and Re^{den} are considered as alleles because there was no recombinant between *Re* and Re^{den} in 504 progeny (Eicher and Varnum 1986). On the other hand, there was one recombinant between *Bsk* and *Re* in 811 progeny (Lyon and Zenthon 1986, 1987). Since no recombination between *Krt1-10* and *Re* was detected in 239 progeny, it was proposed that mutations at *Re* and *Bsk* affecting skin and hair development might involve *Krt1* (Nadeau et al. 1989).

It is well known that mutations in keratin genes cause several human diseases (Lane 1994; Coulombe et al. 1991; Vassar et al. 1991; Cheng et al. 1992; Reis et al. 1994; Mclean et al. 1995). Lesions in a given disease are closely related to the expression sites of keratin genes. In this context, it is considered highly likely that genes in *Krt1*, especially *Krt1-12*, are responsible for the Re^{den} and *Bsk* mutations, because *Krt1-12* is expressed in corneal epithelium (Liu et al. 1993) and is mapped close to the above two mutations on Chr 11 (Liu et al. 1994).

In addition to *Krt1*, *Grn*, a gene encoding the granulin/epithelin precursor (acrogranin), was recently proposed as a possible candidate for Re^{den} and *Bsk*, not only because it was mapped to the same region as *Re* and *Bsk* (Bucan et al. 1996), but because epithelins play important roles in epithelial homeostasis (Shoyab et al. 1990; Plowman et al. 1992).

The mouse mutation, recombination-induced mutation 3 (*Rim3*), arose spontaneously in an intra-MHC recombinant strain, B10.BR(R228), which has a recombinational breakpoint at the *Lmp2* gene in the MHC class II region (Shiroishi et al. 1991). *Rim3* exhibits corneal opacity as well as abnormal skin and hair development. In this report, we carried out more detailed histological analysis of *Rim3* in comparison with Re^{den}, and found that *Rim3* resembles Re^{den} from the neonatal to the adult stage. We also conducted a large-scale linkage analysis of *Rim3*, based on intersubspecific backcrosses. The result indicated that *Rim3* is tightly linked to *Rara* and that many genes including *Krt1-10, 12,* and *Grn,* were excluded as candidates for *Rim3*. The present linkage analysis also revealed that there is a cluster of genes that control growth and differentiation of epithelial cells in a short segment on Chr 11.

Materials and methods

Mice. Rim3 mutant arose spontaneously in an intra-MHC recombinant strain, B10. BR(R228), in the mouse facility at the National Institute of Genetics (NIG) (Mishima, Japan). *Rim3* was introduced to C57BL/10J background (Fig. 1a) and maintained by backcrossing to C57BL/10J (hereinafter abbreviated as B10) purchased from The Jackson Laboratory (Bar Harbor, Me., USA). MSM is an inbred strain established from the Japanese wild mouse (Moriwaki 1994) and maintained at NIG. JF1 is also an inbred strain established from Japanese fancy mice and maintained at NIG. C57BL/6J-$Re^{den/+}$ (Fig. 1b) was a gift from H. Sasaki of the University of Kyushu (Fukuoka, Japan), and maintained by backcrossing to C57BL/6J (hereinafter abbreviated as B6) purchased from The Jackson Laboratory. DBA/2J mice were purchased from CLEA Japan (Tokyo, Japan).

Linkage analysis. Mice for linkage analysis were generated from two different crosses: cross I, (B10-*Rim3*/+ × MSM)F_1 × B10 and B10 × (B10-*Rim3*/+ × MSM)F_1; cross II, (B10-*Rim3*/+ × JF1)F_1 × B10 and B10 × (B10-*Rim3*/+ × JF1)F_1. The resultant progeny were scored for sparse hair at the stage of weaning, indicative of the *Rim3*/+ genotype. Genomic DNA was prepared from liver of the mice and used for linkage analysis. Microsatellite markers were purchased from Research Genetics (Huntsville, Ala., USA), and microsatellite marker *D11Jpk3* was previously reported (Suda et al. 1994). The sequences of oligonucleotide primers for *Krt1-10, Krt1-12,* and *Grn* were set as follows. Krt1-10 F, 5′-CCATGTCTGTTC-TATACAGC-3′ and Krt1-10 R, 5′-CCTGCCCCTTAAGGTCCTCG-3′ (Krieg et al. 1985). The primers amplified a fragment corresponding to the first exon of *Krt1-10* gene. Krt1-12 F, 5′-GTGCACAAGACAGTCCT-GAA-3′ and Krt1-12 R, 5′-CGTGTGAGGCCTTACATCTC-3′ (Liu et al. 1994). The primers amplified a fragment corresponding to the part of the seventh intron and the eighth exon of *Krt1-12* gene. Grn F, 5′-

Correspondence to: T. Shiroishi

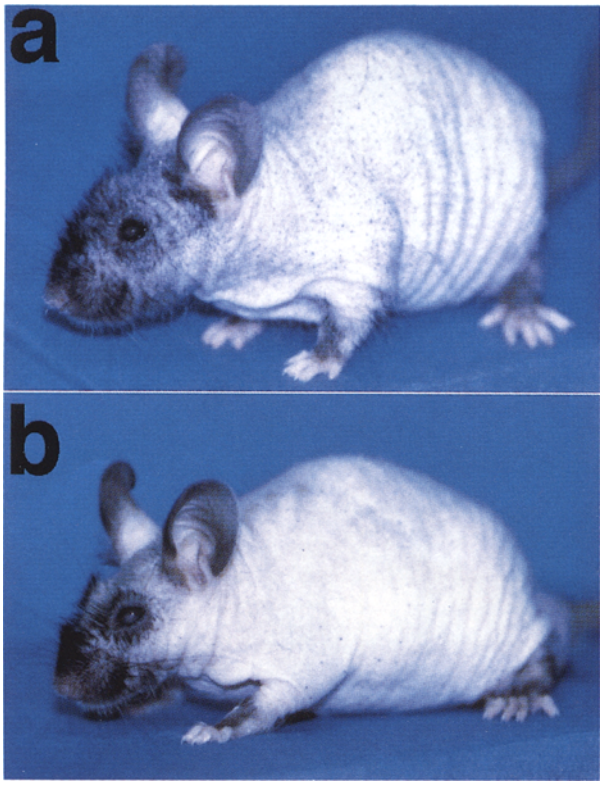

Fig. 1. Phenotype of B10-*Rim3*/+ at 5 months of age **(a)** and B6-Re^{den}/+ at 10 months of age **(b).** Note that both mutants exhibit corneal opacity as well as abnormal skin and hair development.

GCTCCAATAAAGTTTGTACAC-3′ and Grn R, 5′-GCGATCCTG-GAGACTAGAGG-3′ (Baba et al. 1993). The primers amplified a fragment corresponding to the 3′ non-coding region of *Grn* gene. One hundred ng of genomic DNA was amplified by polymerase chain reaction (PCR) according to protocols provided by the manufacturer. Simple sequence length polymorphism (SSLP) was visualized by staining with ethidium bromide on 4% gel (3:1 ratio Nusieve:SeaKem agarose; FMC BioProducts, Rockland, Me., USA) electrophoresis. The PCR products amplified with *Krt1-10* primers were subjected to single-strand conformation polymorphism (SSCP) analysis. For SSCP, heat-denatured samples were electrophoresed on polyacrylamide gel and were visualized by silver staining. The linkage analysis was performed with the Map Manager v2.6.5 and QTB11 programs (Manly 1993). The mapping data from this study are deposited in MGD. The MGD accession number is MGD-JNUM-42692.

Southern analysis. High-molecular-weight DNA was prepared from liver and digested with appropriate restriction enzymes. Digested DNA was electrophoresed on 0.7% agarose and blotted onto nylon membranes (Hybond-N^+; Amersham, Buckinghamshire, UK). Southern hybridization with *Jup* and *Rara* probes was performed by the standard methods (Sambrook et al. 1989). Autoradiograms were analyzed with the BAS2000 Bioimage Analyzer, Fuji Photo Film (Tokyo, Japan). The probe for *Jup* was a 0.5-kb *Sac*I-*Hin*dIII fragment corresponding to the 5′ end of the 2.8-kb cDNA clone of the plakoglobin gene (Butz et al. 1992). The probe for *Rara* was a 1.4-kb *Kpn*I fragment of mouse retinoic acid receptor alpha cDNA cloned by Giguere and coworkers (1990).

Histological analysis. We analyzed F_2 progeny from the intercross of (B10-*Rim3*/+ × DBA/2J)F_1 in order to ascertain the genotype of the mice. Genotypes of the F_2 progeny were determined by SSLP with the microsatellite markers *D11Mit67* and *D11Mit99,* which were located to the proximal and distal region to *Rim3.* Eyeballs and dorsal skin, which were dissected from the mice at different ages (1 day, 1 week, 1 month, and adult), were fixed in 4% paraformaldehyde overnight. After fixation, the tissues were dehydrated, embedded in paraffin, sectioned (eyeball at 3 μm, dorsal skin at 7 μm), and stained with hematoxylin and eosin. Specimens of mutants were compared with the wild type in the same littermates.

Results

Genetic linkage map of Rim3 locus. We obtained a total of 2212 progeny from the two intersubspecific crosses. As a result of linkage analysis, it appeared that *Rim3* was flanked by the proximal marker, *D11Jpk3,* and the distal marker, *D11Mit329.* Out of 2212 backcross progeny, there were 38 and 22 recombinants between the above two markers in crosses I and II, respectively. We carried out haplotype analysis for DNA samples of all 60 recombinants (Fig. 2). Restriction fragment length polymorphisms (RFLPs) for *Jup* and *Rara* were analyzed by Southern blot hybridization with the respective probes. When the recombinant DNA samples were digested with *Kpn*I, the *Jup* probe allowed identification of a polymorphism (19 kb for B10, and 15 kb for MSM and JF1). When the same DNA samples were digested with *Taq*I, a polymorphism (4.5 kb for B10, and 5.4 kb for MSM and JF1) was observed with the *Rara* probe.

We calculated genetic distances between the genes and the microsatellite marker loci from the haplotype analysis (Fig. 3). As

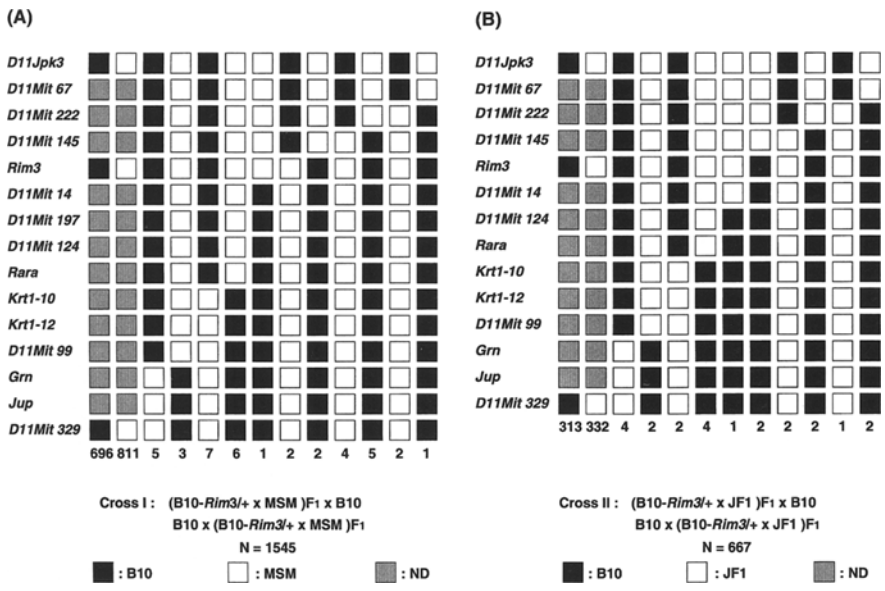

Fig. 2. **(A)** Haplotype analysis of 1545 progeny of Cross I: (B10-*Rim3*/+ × MSM)F_1 × B10 and B10 × (B10-*Rim3*/+ × MSM)F_1. **(B)** Haplotype analysis of 667 progeny of Cross II: (B10-*Rim3*/+ × JF1)F_1 × B10 and B10 × (B10-*Rim3*/+ × JF1)F_1. *Krt1-10, Krt1-12, Grn, Rara, Jup,* and microsatellite marker loci in the present linkage analysis are listed at the left side. Each column represents a chromosomal haplotype identified in the progeny of each cross. The black box indicates the B10 allele, the white box indicates the MSM allele (A), and the JF1 allele (B) and the gray box indicates that the genotype was not determined (ND).

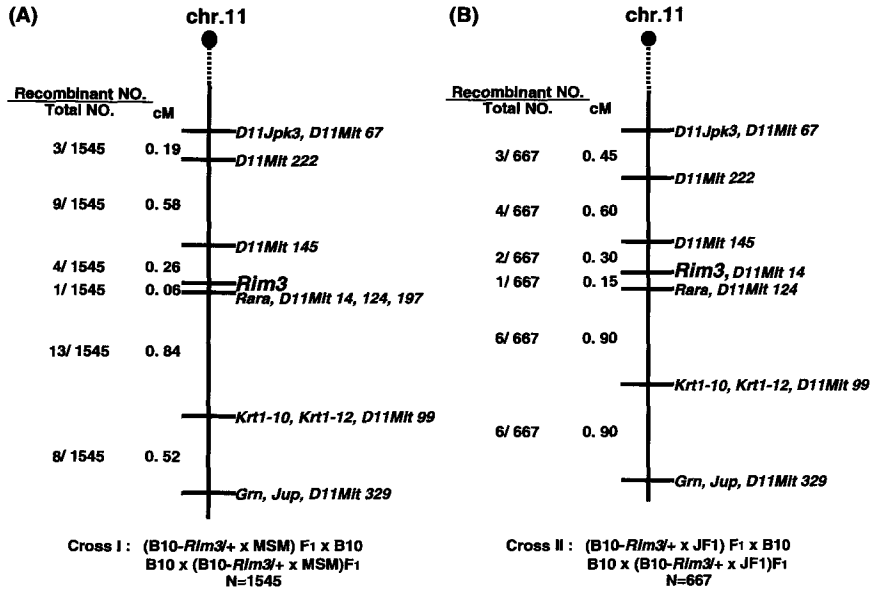

Fig. 3. Genetic maps around *Rim3* locus in Cross I **(A)** and Cross II **(B)**. The map distances (in cM) were shown at the left side of the map.

a result, we found that both *Jup* and *Rara* recombined with *Rim3,* and that *Rim3* gene was flanked by microsatellite markers, *D11Mit145* and *D11Mit14,* on mouse Chromosome 11, with only one recombinant between *Rim3* and *Rara* in each cross. Fourteen and seven recombinants were detected between *Rim3* and *Krt1-10, Krt1-12* in cross I and cross II, respectively, suggesting that *Rim3* and *Krt1-10, Krt1–12* were separated by 0.90 cM and 1.05 cM in the respective cross. Likewise, 22 and 13 recombinants were detected between *Rim3* and *Grn* in cross I and cross II. *Jup* did not recombine with *Grn* and *D11Mti329* in either crosses.

Histological analysis of Rim3 and Re^{den}. To determine whether there are differences in the phenotypes of *Rim3* and Re^{den}, we performed a histological analysis of the dorsal skin and eye at the light microscopy level. F_2 progeny from the intercross of (B10-*Rim3*/+ × DBA//2J)F_1 were genotypically determined by the microsatellite markers *D11Mit67* and *D11Mit99.* Similarly, F_2 progeny from the intercross of (B6-Re^{den}/+ × DBA/2J)F_1 were genotyped by the same microsatellite markers.

In the adult stage of the *Rim3* mutants, abnormalities were observed in the epidermis [Fig. 4(A)-b, c]. Both heterozygotes and homozygotes exhibited mild hyperkeratosis, acanthosis, and hypergranulosis in the epidermis. Few hair follicles were seen in the epidermis of mutant mice. In addition, striking morphological abnormalities were seen in the architecture of the cornea of *Rim3* homozygotes. Aberrations were especially remarkable at the center of the cornea. As seen in Fig. 4(A)-f, homozygotes exhibited hyperkeratosis, acanthosis, hypergranulosis in the epithelial layer, contraction of collagen fibers, infiltration of inflammatory cells in the stromal layer, and severe granulation at the subepithelial portion. Homozygotes revealed corneal lesions earlier than heterozygotes [Fig. 4(A)-e], but heterozygotes also eventually developed the same morphological abnormalities (data not shown).

Similar morphological abnormalities were observed in the epidermis and cornea of the adult stage of Re^{den} mutants as were observed in adult stage of *Rim3* mutants [Fig. 4(B)]. The number of hair follicles was also markedly reduced in the epidermis of mutant mice. Interestingly, hyperplasia of the external root sheath of the hair follicle was observed [Fig. 4(B)-b].

Histological analysis of the cornea and epidermis was carried out in *Rim3* mutants at different ages. The initial morphological alterations in the cornea could be traced back to about 3 months of age. Basal cells of epithelial layer at the center of the cornea of *Rim3* mutants were flat-shaped compared with those of control mice [Fig. 5(A)-b], but the same changes were not detected at the periphery of the cornea. The stromal layer at the center of the cornea was thickened before the epithelial cells were markedly hyperstratified [Fig. 5(A)-c]. At the light microscopy level, early epidermal changes in *Rim3* mutants could be detected at 1 week after birth. The epidermis of mutant mice was slightly thickened at this stage [Fig. 5(B)-a, b, c], and the alteration was apparently observed at 1 month of age [Fig. 5(B)-d, e, f]. However, the number of hair follicles was not significantly reduced at this stage although the external root sheaths of the hair follicles were slightly hyperplastic.

Discussion

In the present linkage analysis based on large-scale intersubspecific backcrosses, the *Rim3* gene is finely mapped to the distal portion, very close to the *Rara* gene, on mouse Chr 11. Mutants Re^{den} and *Bsk,* bearing a marked resemblance to *Rim3,* have been previously mapped to this region. The histological analysis indicated that the main lesions in *Rim3* are almost identical to those in Re^{den}, suggesting that *Rim3* and Re^{den} are allelic. However, we need further investigations to reveal whether *Rim3* is allelic to *Bsk.* Several genes that are related to growth and differentiation of epithelial cells have been mapped to the distal portion of Chr 11. In this study, we also examined whether *Grn, Jup,* and *Krt1* genes could be candidates for *Rim3.*

Grn, the gene encoding the granulin/epithelin precursor (acrogranin) that is processed to the peptides epithelin 1 and epithelin 2, was previously mapped to the distal portion of mouse Chr 11 (Bucan et al. 1996). Epithelin 1 stimulates the proliferation of murine keratinocytes, the major cell type of stratified squamous epithelia, whereas epithelin 2 inhibits the epithelin 1-elicited growth of these cells (Shoyab et al. 1990; Plowman et al. 1992). Taking these functions of epithelins into consideration, mutations in *Grn* may affect architecture of tissue such as the cornea and skin. The present study, however, clearly excluded *Grn* as a candidate for *Rim3.*

Transgenic mice expressing truncated desmoglein 3 exhibited histological similarities to *Rim3* and Re^{den}. Thickened epidermis with marked increase in spinous and stratum corneum layers was shown in the regions where desmosome loss was prevalent, but some adhesive structures remained (Allen et al. 1996). It was assumed that epidermal hyperproliferation is a reaction to the reduction in cell adhesion. Thus, another possible candidate gene for

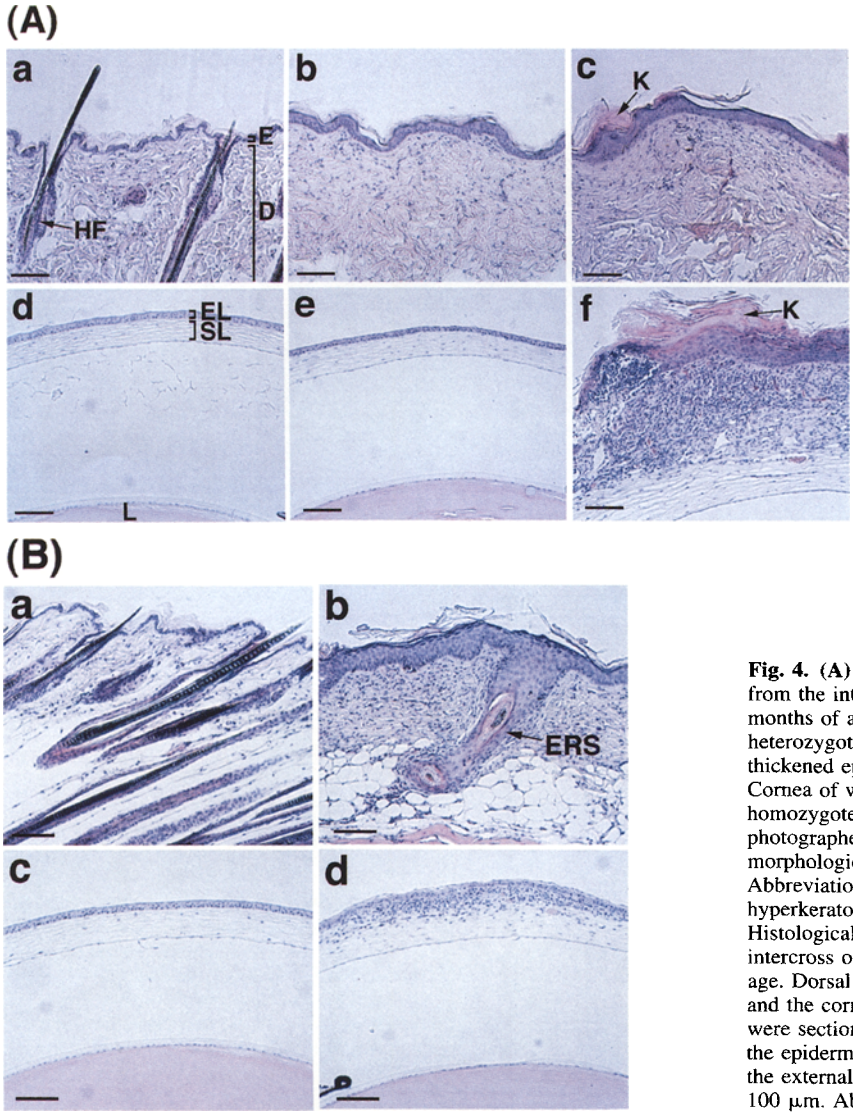

Fig. 4. **(A)** Histological analysis of *Rim3* mutants. Mice generated from the intercross of *Rim3* heterozygotes were examined at 4.5 months of age. Dorsal skin of wild-type mouse (a), the heterozygote (b), and the homozygote (c) were sectioned. Note the thickened epidermis and few hair follicles in mutant mouse. Cornea of wild-type mouse (d), the heterozygote (e), and the homozygote (f) were sectioned at the center of cornea and photographed at same magnification. Note the marked morphological alterations in the homozygote cornea. Bar, 100 μm. Abbreviations: E, epidermis; D, dermis; HF, hair follicle; K, hyperkeratosis; EL, epithelial layer; SL, stromal layer; L, lens. **(B)** Histological analysis of Re^{den} mutants. Mice generated from the intercross of Re^{den} heterozygotes were examined at 4 months of age. Dorsal skin of wild-type mouse (a) and the heterozygote (b) and the cornea of wild-type mouse (c) and the heterozygote (d) were sectioned. Note the similar morphological abnormalities in the epidermis and cornea as seen in *Rim3* mutants. Note also that the external root sheath of the hair follicle was hyperplastic. Bar, 100 μm. Abbreviation: ERS, external root sheath.

Rim3 is the junctional plakoglobin (*Jup*) gene, because *Jup* encodes the common plaque protein for two major types of adhering junctions, adherens junctions and desmosomes, in epithelial cells (Schmidt et al. 1994), and it was mapped to the distal region on Chr 11 (Guénet et al. 1995). In this study, *Jup* is colocalized to *D11Mit329* and separated from *Rim3*.

Retinoids are known to have an important effect on epithelial differentiation. They enhance differentiation of simple epithelia, but inhibit terminal differentiation of epidermis and other stratified squamous epithelia. When epidermal cells were grown in the absence of vitamin A, they showed reduced motility and no tendency to discharge from the upper surface of the epithelium, although they revealed terminal differentiation (Fuchs and Green 1981). Epidermal cells and epithelial cells at the center of the cornea in *Rim3* and Re^{den} were hyperstratified with hyperkeratosis and hypergranulosis. These phenotypes might be caused by disturbance of action of vitamin A. Retinoic acid receptor alpha (*Rara*) was previously mapped near homeobox-2 complex and the *Krt1* on mouse Chr 11 (Nadeau et al. 1992). The present data revealed genetic evidence that *Rim3* and *Rara* were very tightly linked but were separated.

Keratin proteins form the intermediate filament cytoskeletal network in epithelial cells. These are classified into two families, type I and type II (Moll et al. 1982; Eichner et al. 1984; Steinert and Roop 1988). On the basis of expression sites (Fuchs and Green 1980; Liu et al. 1993), as well as the chromosomal location, the *Krt1-12* gene, which is included in *Krt1* and is expressed in corneal epithelium, has been proposed to be responsible for Re^{den}. Our mapping study excluded this gene as a candidate for *Rim3*. In the present study, another gene in *Krt1, Krt1-10,* was also excluded as a candidate for *Rim3*. The human disease, epidermolytic hyperkeratosis (EH), is caused by mutations in human KRT10, which is expressed in suprabasal cells of the epidermis. Degenerative and lysed suprabasal cells and hyperthickened stratum corneum are recognized in EH. Therefore, absence of degenerative and lysed suprabasal cells in epidermis of *Rim3* and Re^{den} supports the assumption that mouse *Krt1-10* is not involved in the mutations, which is consistent with our linkage analysis.

On the cornea, the most early change observed in *Rim3* mutants was flat-shaped basal epithelial cells only at the center of the cornea where aberrations would be exacerbated [Fig. 5(A)-b]. It was reported that transforming growth factor alpha (*Tgfa*) knockout mice displayed waviness of the whiskers and fur, and often eye abnormalities including corneal inflammation and scarring (Bruce Mann et al. 1993; Luetteke et al. 1993). In these mice, basal epithelial cells in the cornea were flat-shaped, and inflammatory cells infiltrated into the stromal layer. These observations suggested the possibility that the *Rim3* gene may be closely related to the growth factor necessary for corneal integrity.

As shown in Fig. 5B, epidermal hyperstratification preceded

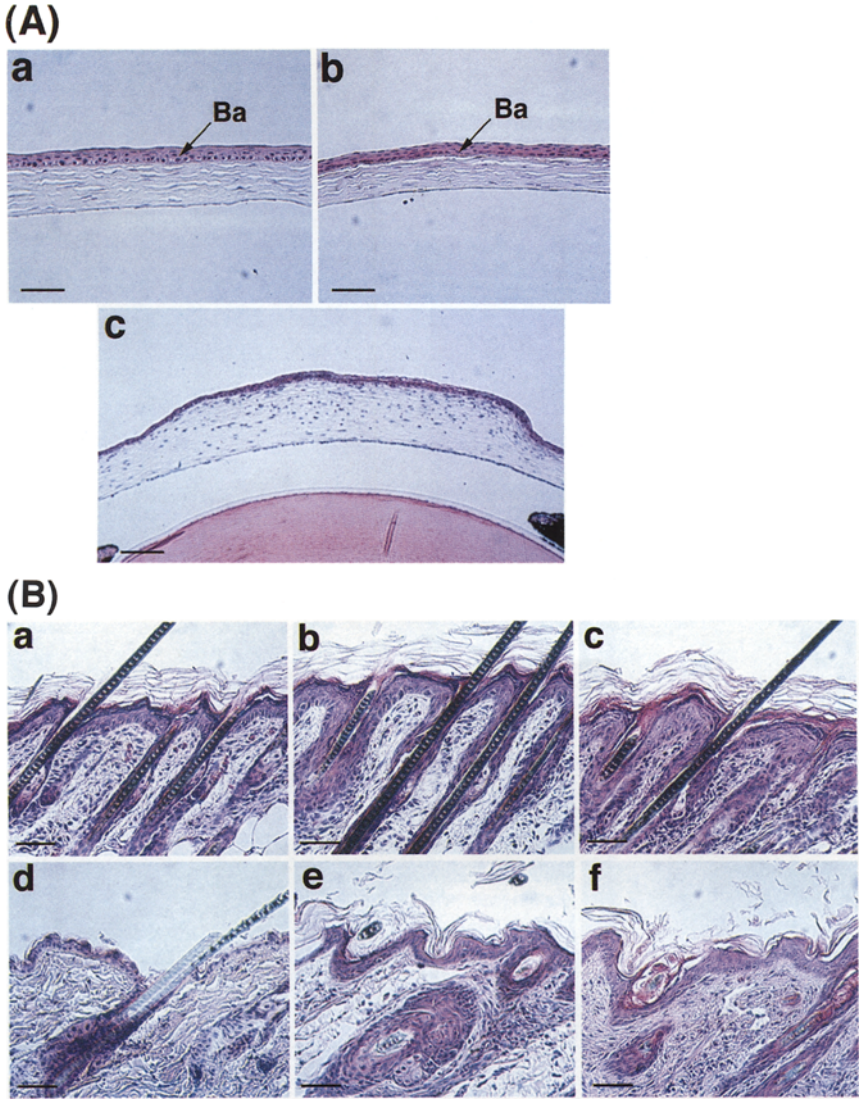

Fig. 5. **(A)** Morphological changes in the cornea of *Rim3* mutants. Section of the center of the cornea of wild-type mouse (a), *Rim3* heterozygote at 3 months of age showing flat-shaped basal cells of the epithelial layer (b), and *Rim3* homozygote at 3 months of age showing thickened stromal layer with disorganized epithelial layer (c). Bar, 50 μm in (a), (b); 100 μm in (c). Abbreviation: Ba, basal cell. **(B)** Morphological changes in the skin of *Rim3* mutants. Wild-type mouse (a), (d); *Rim3* heterozygote (b), (e); *Rim3* homozygote (c), (f). Sections of the dorsal skin at 1 week of age (a), (b), (c), and at 1 month of age (d), (e), (f). Note that the epidermis of mutant mouse was slightly thickened at 1 week of age and was clearly thickened at 1 month of age. However, the number of hair follicles was not reduced at this stage. Bar, 50 μm.

hair loss. It is known that once the hair follicle is established, hair growth is cyclic. In the bulge activation hypothesis, a new hair cycle is thought to be started by activation of the bulge where follicular stem cells reside by dermal papilla (Cotsarelis et al. 1990). In *Rim3* mutants, it is mostly suspected that the bulge may be gradually disorganized as epidermis thickens because the bulge is a specific area of external root sheath of the hair follicle in which the cells are contiguous with the basal layer of epidermis. That may be the reason that hair loss of *Rim3* mutants gradually progresses.

We have undertaken fine mapping of *Rim3,* using two kinds of intersubspecific backcrosses for prevention of distortion of recombination frequency depending on the strains used in the cross. The present mapping data showed unambiguous gene order and almost the same recombination frequencies between two different crosses. Moreover, it turned out that *D11Mit14* was most tightly linked to *Rim3,* as shown in crosses I and II, and would be a useful marker for positional cloning of the *Rim3* gene. Finally, it is notable that many functionally related genes such as *Grn, Jup, Rara, Krt1,* and *Rim3,* are located within a short segment in the distal portion of mouse Chr 11. This suggests that the region consists of a functional domain to control growth and differentiation of epithelial cells.

Acknowledgments. We are grateful to Dr. Rolf Kemler (Max-Planck-Institut für Immunbiologie) and Dr. Vincent Giguere (Molecular Oncology Group, McGill University, Royal Victoria Hospital) for their kind gifts of probes. We thank Dr. Hiroyuki Sasaki (University of Kyushu) for giving us Re^{den} mice, and also Ms. Keiko Shimizu for her assistance in DNA preparation and linkage analysis. We also thank Dr. Kazuo Moriwaki for establishing MSM and JF1 strains and encouragement during the course of this study. This study was supported in part by grants-in-aid from the Ministry of Education, Science, and Culture of Japan. This study is contribution number 2099 from the National Institute of Genetics, Mishima, Japan.

References

Allen E, Yu Q-C, Fuchs E (1996) Mice expressing a mutant desmosomal cadherin exhibit abnormalities in desmosome, proliferation, and epidermal differentiation. J Cell Biol 133, 1367–1382

Baba T, Nemoto H, Watanabe K, Arai Y, Gerton GL (1993) Exon/intron organization of the gene encoding the mouse epithelin/granulin precursor (acrogranin). FEBS Lett 322, 89–94

Bruce Mann G, Fowler KJ, Gabriel A, Nice EC, Williams RL, Dunn AR (1993) Mice with a null mutation of the TGF α gene have abnormal skin architecture, wavy hair, and curly whiskers and often develop corneal inflammation. Cell 73, 249–261

Bucan M, Gatalica B, Bata T, Gerton GL (1996) Mapping of *Grn,* the gene encoding the granulin/epithelin precursor (acrogranin), to mouse Chromosome 11. Mamm Genome 7, 704–713

Butz S, Stappert J, Weissig H, Kemler R (1992) Plakoglobin and β-catenin: distinct but closely related. Science 257, 1142–1144

Cheng J, Syder AJ, Yu Q-C, Letai A, Paller AS, Fuchs E (1992) The genetic basis of epidermolytic hyperkeratosis: a disorder of differentiation-specific epidermal keratin genes. Cell 70, 811–819

Cotsarelis G, Sun T-T, Lavker RM (1990) Label-retaining cells reside in the bulge area of pilosebaceous unit: implications for follicular stem cells, hair cycle, and skin carcinogenesis. Cell 61, 1329–1337

Coulombe PA, Hutton ME, Letai A, Hebert A, Paller AS, Fuchs E (1991) Point mutations in human keratin 14 genes of epidermolysis bullosa simplex patients: genetic and functional analyses. Cell 66, 1301–1311

Eicher EM, Varnum D (1986) Allelism of Den and Re. Mouse News Lett 75, 29–30

Eichner R, Bonitz P, Sun T-T (1984) Classification of epidermal keratins according to their immunoreactivity, isoelectric point, and mode of expression. J Cell Biol 98, 1388–1396

Fuchs E, Green H (1980) Changes in keratin gene expression during terminal differentiation of the keratinocyte. Cell 19, 1033–1042

Fuchs E, Green H (1981) Regulation of terminal differentiation of cultured human keratinocytes by vitamin A. Cell 25, 617–625

Giguere V, Shago M, Zirngibl R, Tate P, Rossant J, Varmuza S (1990) Identification of a novel isoform of the retinoic acid receptor γ expressed in mouse embryo. Mol Cell Biol 10, 2335–2340

Green MC (1989) Catalog of mutant genes and polymorphic loci. In *Genetic Variants and Strains of the Laboratory Mouse,* 2nd ed. MF Lyon, AG Searle, eds. (Oxford, UK: Oxford University Press), pp 12–403

Guénet JL, Simon-Chazottes D, Ringwald M, Kemler R (1995) The genes coding for alpha and beta catenin (*Catna1* and *Catnb*) and plakoglobin (*Jup*) map to mouse chromosomes 18, 9, and 11, respectively. Mamm Genome 6, 363–366

Krieg TM, Schafer MP, Cheng CK, Filpula D, Flaherty P, Steinert PM, Roop DR (1985) Organization of a type I keratin gene. J Biol Chem 260, 5867–5870

Lane EB (1994) Keratin diseases. Curr Opin Genet Dev 4, 412–418

Liu C-Y, Zhu G, Westerhausen-Larson A, Converse R, Kao CW-C, Sun T-T, Kao WW-Y (1993) Cornea-specific expression of K12 keratin during mouse development. Curr Eye Res 12, 963–974

Liu C-Y, Zhu G, Converse R, Kao CW-C, Nakamura H, Tseng SC-G, Mui M-M, Seyer J, Justice MJ, Stech ME, Hansen GM, Kao WW-Y (1994) Characterization and chromosomal localization of the cornea-specific murine keratin gene *krt1.12.* J Biol Chem 269, 24627–24636

Luetteke NC, Qiu TH, Peiffer RL, Oliver P, Smithies O, Lee DC (1993) TGF α deficiency results in hair follicle and eye abnormalities in targeted and waved-1 mice. Cell 73, 263–278

Lyon MF, Zenthon JF (1986) Close linkage of bareskin (Bsk) and rex (Re). Mouse News Lett 74, 96.

Lyon MF, Zenthon JF (1987) Relationship between bareskin denuded, and rex. Mouse News Lett 77, 125

Manly K (1993) A Macintosh program for storage and analysis of experimental genetic mapping data. Mamm Genome 4, 301–314

Mclean WHI, Rugg EL, Lunny DP, Morley SM, Lane EB, Swensson O, Dopping-Hepenstall PJC, Griffiths WAD, Eady RAJ, Higgins C, Navsaria HA, Leigh IM, Strachan T, Kunkeler L, Munro CS (1995) Keratin 16 and keratin 17 mutations cause pachyonychia congenita. Nature Genet 9, 273–278

Moll R, Franke WW, Schiller DL, Geiger B, Krepler R (1982) The catalog of human cytokeratins: patterns of expression in normal epithelia, tumors, and cultured cells. Cell 31, 11–24

Moriwaki K (1994) Wild mouse from a geneticist's viewpoint. In *Genetics in Wild Mice,* K Moriwaki T, Shiroishi H, Yonekawa, eds. (Tokyo/Basel: Japan Scientific Society Press/Karger), pp. xiii-xxv.

Nadeau, JH, Berger FG, Cox DR, Crosby JL, Davisson MT, Ferrara D, Fuchs E, Hart C, Hunihan L, Lalley PA, Langley SH, Martin GR, Nichols L, Phillips SJ, Roderick TH, Roop DR, Ruddle FH, Skow LC, Compton JG (1989) A family of type I keratin genes and the homeobox-2 gene complex are closely linked to the rex locus on mouse chromosome 11. Genomics 5, 454–462

Nadeau JH, Compton JG, Giguere V, Rossant J, Varmuza S (1992) Close linkage of retinoic acid receptor genes with homeobox- and keratin-encoding genes on paralogous segments of mouse chromosomes 11 and 15. Mamm Genome 3, 202–208

Plowman GD, Green JM, Neubauer MG, Buckley SD, McDonald VL, Todaro GJ, Shoyab M (1992) The epithelin precursor encodes two proteins with opposing activities on epithelial cell growth. J Biol Chem 267, 13073–13078

Reis A, Hennies H-C, Langbein L, Digweed M, Mischke D, Drechsler M, Schrock E, Royer-Pokora B, Franke WW, Sperling K, Kuster W (1994) Keratin 9 gene mutations in epidermolytic palmoplantar keratoderma (EPPK). Nature Genet 6, 174–179

Sambrook J, Fritsch EF, Maniatis T (1989) *Molecular Cloning: A Laboratory Manual,* 2nd ed. (Cold Spring Harbor, NY: Cold Spring Harbor Laboratory Press)

Schmidt A, Heid HW, Schafer S, Nuber UA, Zimbelmann R, Franke WW (1994) Desmosomes and cytoskeletal architecture in epithelial differentiation: cell type-specific plaque components and intermediate filament anchorage. Eur J Cell Biol 65, 229–245

Shiroishi T, Sagai T, Hanzawa N, Gotoh H, Moriwaki K (1991) Genetic control of sex-dependent meiotic recombination in the major histocompatibility complex of the mouse. EMBO J 10, 681–686

Shoyab M, McDonald VL, Byles C, Todaro GJ, Plowman GD (1990) Epithelin 1 and 2: isolation and characterization of two cysteine-rich growth-modulating proteins. Proc Natl Acad Sci USA 87, 7912–7916

Steinert PM, Roop DR (1988) Molecular and cellular biology of intermediate filaments. Annu Rev Biochem 57, 593–625

Suda T, Oyanagi M, Wakana S, Takahashi Y, Kanada H, Yonekawa H, Miyashita N, Shiroishi T, Moriwaki K, Kominami R (1994) Novel mouse microsatellites: primer sequences and chromosomal location. DNA Res 1, 169–174

Vassar R, Coulombe PA, Degenstein L, Albers K, Fuchs E (1991) Mutant keratin expression in transgenic mice causes marked abnormalities resembling a human genetic skin disease. Cell 64, 365–380